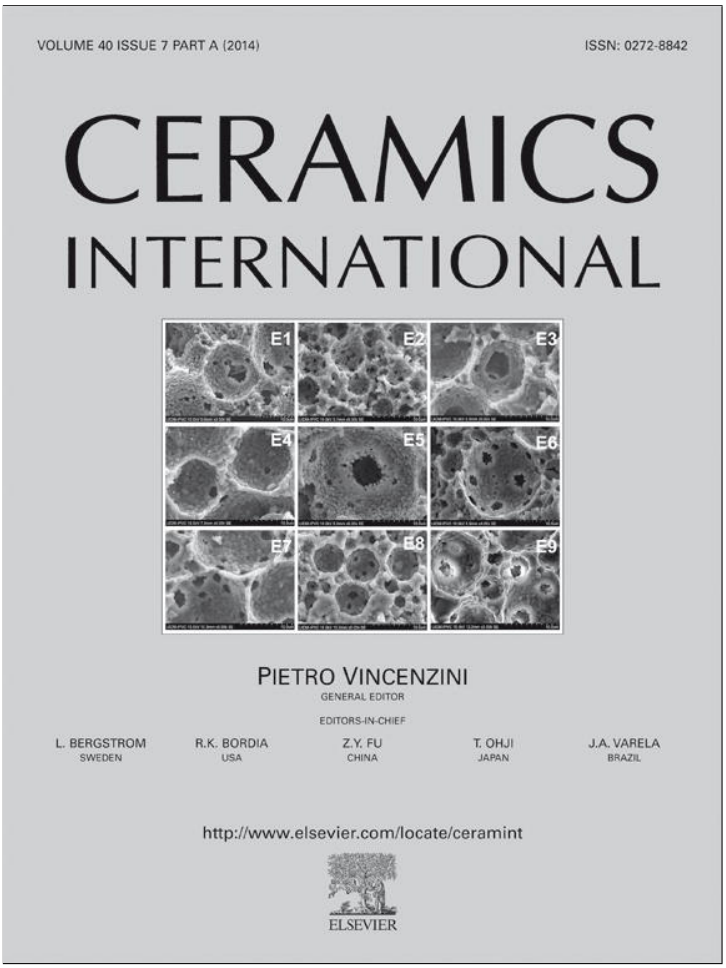

Available online at www.sciencedirect.com

ScienceDirect

Ceramics International 40 (2014) 9583–9589

CERAMICS INTERNATIONAL

www.elsevier.com/locate/ceramint

Effect of capillary action on bone regeneration in micro-channeled ceramic scaffolds

Daniel S. Oh[a,*,1], Young Joon Kim[a,b,1], Min-Ho Hong[a], Myung-Ho Han[c], Kyungsoo Kim[d,**]

[a]*Columbia University, Center for Orthopaedic Research, New York, NY, USA*
[b]*Trinity School, New York, NY, USA*
[c]*Department of Chemical Engineering, Kyungil University, Gyeongsan, Republic of Korea*
[d]*Department of Applied Mathematics, Kyung Hee University, 1732 Deogyeong-daero, Giheung-gu, Yongin-si, Gyeonggi-do 446-701, Republic of Korea*

Received 7 January 2014; received in revised form 8 February 2014; accepted 9 February 2014
Available online 24 February 2014

Abstract

A new scaffold design was introduced with macro-pores and micro-channels, which greatly assisted in the initial bone marrow absorption and uniform cell distribution. Unfortunately, the underlying scientific reasons for the new scaffold's efficiency are currently unknown. Hence, we approached using a mathematical and experimental method to elucidate the new scaffold's efficiency. The mathematical formula describe rising fluid height in a narrow cylindrical vessel due to capillary action. Through the mathematical simulation, the maximum fluid heights at equilibrium for scaffold tubes of diameters 50, 150, 350, and 750 μm were 156.6, 52.7, 22.6, and 10.5 mm, respectively. The fluid would theoretically reach 90% of the maximum height at 900, 30, 3, and 0.3 s, respectively. In the experiment, the fluid heights were observed from 30 to 600 s. All the scaffolds had 50 μm micro-channels with different macro-pore sizes of 150, 350, and 750 μm. The media rose through macro-pores of the three scaffolds until 40, 15, and 10 mm, respectively. The fluid heights were observed at about 2 s and 0.5 s after being immersed for the 350 μm and 750 μm macro-pore scaffolds. In the case of the 150 μm sample, the fluid height was 30 mm at about 30 s and 40 mm at about 75 s. Since all samples had 50 μm micro-channels, the fluid reached to the top of the scaffolds, eventually. The results showed that capillary action was highly dependent on the size of the tubes within the scaffold. They also confirmed the simulated data in both equilibrium height and the time trajectory. The data from both the experiment and the mathematical simulation proved our hypothesis that capillary action was the cause for the improvement in cell immigration in the new scaffold since the data matched each other in both equilibrium height and the time trajectory.

Keywords: Absorption; Bone regeneration; Capillary action; Distribution; Micro-channel

1. Introduction

Bones are important vital components of the skeletal system. They serve numerous functions such as protecting important organs including brain and heart, body support, moving muscles and joints, storing minerals and fat, acid–base balance, and synthesizing blood cells [1]. Bone defects could occur due to trauma caused by accidents, sports injuries, tumors, osteoporotic fractures, or other diseases and infections [2]. Despite the progress made in bone regeneration in recent years, it still has many clinical obstacles that prevent doctors to comfortably use regenerative techniques on patients. One such advancement is the scaffold, which is an artificial structure capable of supporting three-dimensional bone regeneration. However, treatment of large bone defects is still currently a major clinical dilemma [3]. Therefore, there must be an effective method of bone regeneration so that bone defects and injuries can be successfully treated by orthopedic surgery.

Tissue engineering is the use of a combination of cells, engineering, special materials, and suitable biochemical and

*Correspondence to: Department of Orthopaedic Surgery, Columbia University Medical Center, 650 West 168th street, New York, NY 10032, USA. Tel.: +1 212 305 7965; fax: +1 212 305 2741.
**Corresponding author. Tel.: +82 31 201 2408; fax: +82 31 204 8122.
E-mail addresses: dso2113@columbia.edu (D.S. Oh), kyungsoo@khu.ac.kr (K. Kim).
[1]These authors contributed equally to this work.

http://dx.doi.org/10.1016/j.ceramint.2014.02.033
0272-8842

physio-chemical factors. The goal of using engineered tissue is to replace or restore native tissue functions. Scaffolds are artificial structures capable of supporting three-dimensional tissue formation [4–7]. In order to work correctly, these scaffolds must mimic natural bone characteristics such as pore size, porosity, interconnectivity of the pores, and permeability. If these scaffolds can mimic bone structure accurately, then proper cell attachment, proliferation, differentiation, nutrient flow and cell communication, which are all crucial for proper bone healing, can be achieved [8–11]. Unfortunately, current scaffold structures limit active initial cell infiltration and cell colonization use as they decrease the rate of the diffusion of oxygen and nutrients [12,13]. In order to overcome these limitations, the initial host bone marrow absorption and the quality of nutrient flow into and out of the graft must be improved through a more efficient scaffold design [14].

Recently, a novel hydroxyapatite (HA) ceramic scaffold design with macro-pores and micro-channels was introduced to enhance fluid absorption and retention [14]. This HA-scaffold has a synthetic construction that actively initiates bone marrow absorption and uniform distribution of bone marrow. On the cellular level, this HA-scaffold induced exceptional cell attachment, proliferation, and differentiation on a uniform scale throughout the scaffold. This scaffold also provided several advantages such as histo-morphometry parameters similar to those of the human lumbar vertebrae bone, high surface-area/porosity ratio, successful bone marrow absorption and retention capability, and excellent preliminary mobilization and habitation of cells in in-vitro experiments. However, the underlined scientific principles of the advantages of the micro-channeled scaffold design are not well known.

We hypothesize that hollow channels with micron-scale diameters within the scaffold exhibit highly efficient fluid absorption due to natural phenomenon called “capillary action.” More specifically, we hypothesize that capillary action would exert a fluidic force on attached cells through scaffold's micro-channels, mechanically inducing cell proliferation or differentiation. This study has two purposes. The first purpose is to estimate the maximum height the fluid would reach in samples of scaffolds with different micro-channel diameters by formulating a mathematical model describing capillary action, fluid height, and time. The second purpose is to validate the mathematical model for capillary action by conducting experiments with samples of the actual scaffolds that were matched with the mathematical model's scale.

2. Materials and methods

2.1. Physics of capillary action with real-world examples

Capillary action is the ability of a fluid to flow into narrow spaces (the micro-channels in this experiment) against external forces, such as the pull of gravity, due to cohesive forces between the fluid's molecules and adhesive forces between the fluid's molecules and the molecules of the fluid's container [15,16]. If the diameter of the tube is sufficiently small, then this combination of cohesive and adhesive forces between the liquid and container acts to lift the liquid [16]. There are several examples of the capillary action in the natural world. For example, when the bottom of a piece of paper is dipped in water, the water will actually flow higher than the surface of the water in its container. This happens because there exist very small gaps between the paper fibers into which the water can enter. The polar water molecules are attracted to the paper molecules (there is an adhesive force between them) and as a result of this, the water rises and as the water molecules rise they ‘pull up’ more water molecules with them due to the cohesive forces between the molecules. This process continues until the combination of cohesive and adhesive forces equals the downward pull of gravity. A dry paper towel absorbs liquid by drawing it into the narrow openings between the fibers [17]. The transport of fluids within plants is also an example of capillary action in nature. As the plant releases water from its leaves, water is drawn upward from the roots to replace it. In the human circulatory system, blood movement in microscopic capillaries from arterioles to venules is achieved by capillary action against the blood flowing downward due to gravity [18].

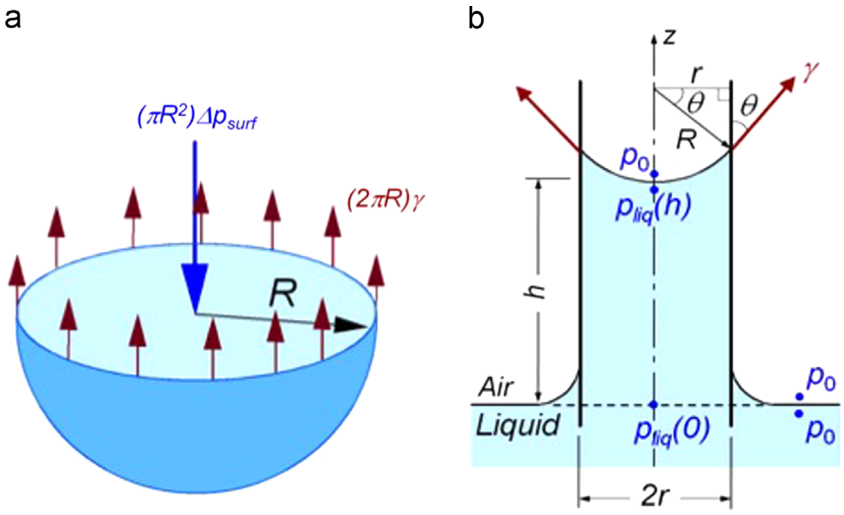

Fig. 1. (a) The free body diagram of half a droplet [19]. (b) The capillary rise in a narrow cylindrical tube [20].

2.2. Mathematical formulation of the capillary action

The basic mathematical formulation used in this study was based on three fluid mechanics books [15,19,20]. Consider a half of a droplet having a radius of curvature R, as shown in Fig. 1(a). A curved liquid–air interface indicates a pressure difference across the interface. The pressure difference, inside Δp_{surf} inside a droplet can be determined by considering the free body diagram of half a droplet. We then have

$$(2\pi R)\gamma = \Delta p_{surf}(\pi R^2), \tag{1}$$

where γ is surface tension.

Denoting with θ the contact angle of the fluid level on the solid wall, Eq. (1) can be expressed as

$$\Delta p_{surf} = \frac{2\gamma}{r}\cos\theta \tag{2}$$

by using $R = r/\cos\theta$ from the geometry.

If we consider the liquid–air interface at the equilibrated capillary rise height of h as shown in Fig. 1(b), the pressure difference Δp_{surf} will be present across the interface, which is given by

$$\Delta p_{surf} = p_0 - p_{liq}(h), \tag{3}$$

where p_0 and $p_{liq}(h)$ denote the air (atmospheric) pressure and the liquid pressure at a level just below a capillary rise height h, respectively. On the other hand, in terms of hydrostatic pressure, the pressure rise at a level with depth of h below the top free surface of liquid inside the tube is equal to ρgh where ρ and g are the density of the fluid and the gravity constant, respectively.

$$p_0 = p_{liq}(0) = p_{liq}(h) + \rho gh \tag{4}$$

From Eqs. (2) and (4), the equilibrium height of h can be expressed as

$$h = \frac{2\gamma\cos\theta}{\rho gr} \tag{5}$$

By using the equilibrium height, h established in Eq. (5), we could now develop the capillary height function with respect to time by solving a differential equation. Let $L(t)$ be the height of the liquid column inside the tube at time, t. The equilibrium is reached at $t\to\infty$ as so $L(\infty) = h$. The speed of the rising liquid, dL/dt, can be found by the average velocity $v_0 = Q/(\pi r^2)$ of the vertical liquid flow inside the tube of radius, r, where Q is the flow rate. Then, assuming that the liquid flow is a fully developed Hagen–Poiseuille flow, the pressure drop in a fluid flowing through a long cylindrical tube Δp is related to the flow rate, Q as follows [20]:

$$Q = \frac{\pi r^4}{8\eta L}\Delta p \tag{6}$$

where η is dynamic viscosity coefficient of liquid. Then, we can obtain the approximate form of the average fluid velocity as follows:

$$\frac{dL(t)}{dt} = v_0 = \frac{Q}{\pi r^2} \approx \frac{r^2\Delta p(t)}{8\eta}\cdot\frac{1}{L(t)} \tag{7}$$

The pressure difference, $\Delta p(t)$, between $h = 0$ and $h = L(t)$, induced by viscous friction in the rising liquid column must equal the Laplace pressure across the meniscus minus the decreasing hydrostatic pressure of the liquid column. This can be expressed as follows:

$$\Delta p(t) = \Delta p_{surf} - \rho gL(t) \tag{8}$$

By inserting Eq. (8) into Eq. (7) with Eqs. (4) and (5) for Δp_{surf}, we get a first-order ordinary differential equation for the capillary rise height, $L(t)$:

$$\frac{dL(t)}{dt} = \frac{r^2}{8\eta L(t)}[\rho gh - \rho gL(t)] = \frac{\rho gr^2}{8\eta}\left[\frac{h}{L(t)} - 1\right] \tag{9}$$

with $L(0) = 0, \quad L(\infty) = h$. We then have the analytical implicit solution of the differential equation as follows:

$$t = -\frac{8\eta}{\rho gr^2}\left(h\ln\left|\frac{L(t)}{h} - 1\right| + L(t)\right) \tag{10}$$

2.3. Numerical simulation with different capillary tube parameters

In order to estimate the maximum height that the fluid reaches and the time it takes in the process, we solved the expression for t in Eq. (10) with respect to $L(t)$. Then, we plotted the height of media fluid with respect to the corresponding time, t, for different scaffold tube diameters. The default material properties and the fluid–scaffold interface parameters used in the simulation are described in Table 1. In the simulation, four different diameters,

Table 1
The material and fluid–scaffold interface parameters used in the numerical simulation.

Variable	Description	Value
γ	Surface tension of blood	0.06 N/m
ρ	Density of blood	1060 kg/m^3
g	Gravity acceleration	9.8 m/s^2
θ	Contact angle	70°
η	Dynamic viscosity of blood	0.00326 Pa s
d	Diameter of the tube	50, 150, 350, 750 μm

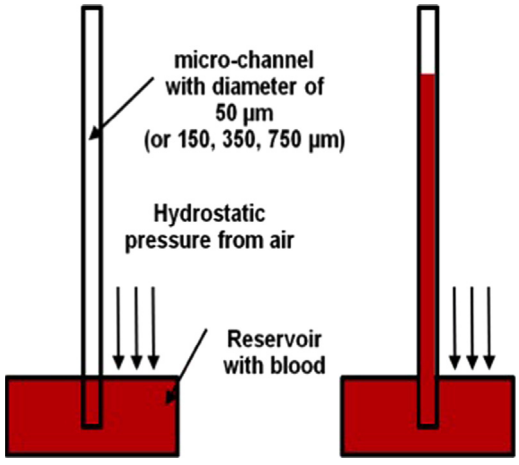

Fig. 2. Schematic diagram of capillary rise tube with different diameters.

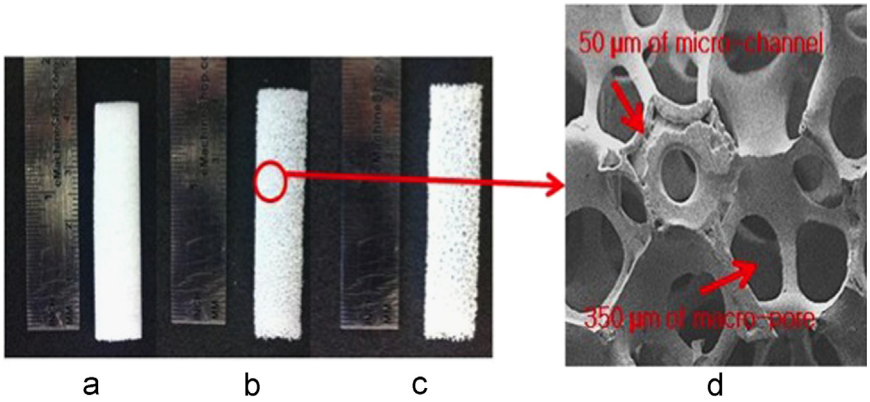

Fig. 3. Three different scaffold specimens were manufactured and used in the experiments for the demonstration of capillary action. (a) 150 μm macro-pore and 50 μm micro-channel scaffold. (b) 350 μm macro-pore and 50 μm micro-channel scaffold. (c) 750 μm macro-pore and 50 μm micro-channel scaffold. (d) 350 μm macro-pore and 50 μm micro-channel scaffold close up. (For interpretation of the references to color in this figure, the reader is referred to the web version of this article.)

50, 150, 350, and 750 μm of the scaffold tube were considered, as shown in Fig. 2.

2.4. Experiments of capillary action using HA-scaffold

We obtained the HA-scaffold specimens with three different scaffold macro-pore sizes 150 μm (100–210 μm), 350 μm (290–420 μm), and 750 μm (690–810 μm) with 50 μm micro-channels in terms of mean diameter, respectively. Each of the six specimens was used to calculate the mean diameter for each group. Fig. 3 shows a picture of the macro-pores with micro-channels inside the scaffold. The two red arrows show the macro-pores and micro-channels clearly.

The dimension of each specimen is 1 cm × 1 cm × 4 cm. We put the HA-scaffold specimen into a 6-well cell-culture plate filled with media. To mimic the blood flow condition, the media viscosity was controlled using glycerol (Sigma-Aldrich, USA) compared with blood viscosity in Table 1. The absorption experiments were performed three times for each group. We then observed the upper boundary of the dark and the light stained areas. The dark stained area specifies the capillary action height limit due to the macro-scaffold pores, while light stained area specifies the capillary action due to the micro-channel inside the scaffold strut.

3. Results

From the mathematical simulation, it is observed that the maximum heights of the fluid at equilibrium status for different scaffold tube of diameters 50 μm, 150 μm, 350 μm, and 750 μm, were 156.6 mm, 52.7 mm, 22.6 mm, and 10.5 mm, respectively, as can be seen in Fig. 4. We also find from Fig. 4 that the fluid reached to 80% of the maximum height at about 500, 20, 1, and 0.1 s for 50 μm, 150 μm, 350 μm, and 750 μm, respectively, and to 90% of the maximum height at about 900, 30, 3, and 0.3 s for 50 μm, 150 μm, 350 μm, and 750 μm, respectively.

Fig. 5 shows the experimental results on the fluid heights (a) at 30 s, (b) at 1 min, (c) at 3 min, (d) at 6 min, and (e) at 10 min. In (f) the final fluid heights inside the three different macro-pores and the micro-channels scaffolds are shown. In the experiments, the scaffold with 150 μm of macro-pores showed a higher capillary line while the scaffold with 750 μm macro-pores showed a lower capillary line (the red lines in Fig. 5(f)). The 150 μm, 350 μm, and 750 μm of macro-pore scaffolds showed 40 mm, 15 mm, and 10 mm of maximum heights in dark stained area (Fig. 5(f) and Table 2). Since the media in the 150 μm macro-pore scaffold reached the maximum height of the scaffold, we can expect that the real maximum height in this case is greater than 40 mm of the scaffolds sample. In addition, the maximum heights were observed at about 2 s and 0.5 s after the start in the cases of 350 μm and 750 μm, while the height was 30 mm at about 30 s and 40 mm at about 75 s in the case of 150 μm. Regrettably, for 150–50 μm combination, the maximum height was overestimated while the time to maximum height was underestimated in the mathematical model as compared to the experimental model. We posit that the 150–50 μm combination has more structure than others which can cause more un-ideal shape and conditions throughout the scaffold. In addition, we were able to create a maximum of 40 mm height scaffold due to the limitations of the equipment. From the result, we found that the capillary action highly depends on the pore (or tube) size. However, the upper parts of the scaffolds, shown as the light stained part, were filled with the media because all three scaffolds have 50 μm of micro-channels. Those additional capillary actions are driven by the micro-channels. The results obtained from the experiments confirmed our mathematical simulation of capillary action in these channels in terms of not only the maximum height but also the time trajectory to reach the maximum height.

4. Discussion

The goals of engineered tissue scaffolds are to integrate with host bone to recruit the host cells and to allow an active exchange of ions, gas, and fluids [6]. Various materials of scaffolds have been used such as polymers, ceramics, metals, or other composite materials in order to achieve some biocompatibility and mechanical strength [14]. The micro-channeled HA-scaffold has demonstrated enhanced bone marrow absorption and retention properties when

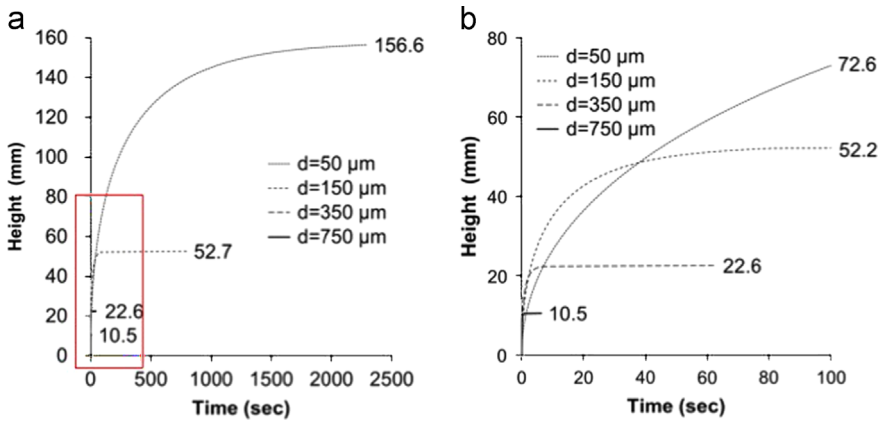

Fig. 4. Capillary heights vs. time for different scaffold tube diameters: the capillary heights are plotted (a) for the time duration of 2500 s and (b) only for the beginning 100 s.

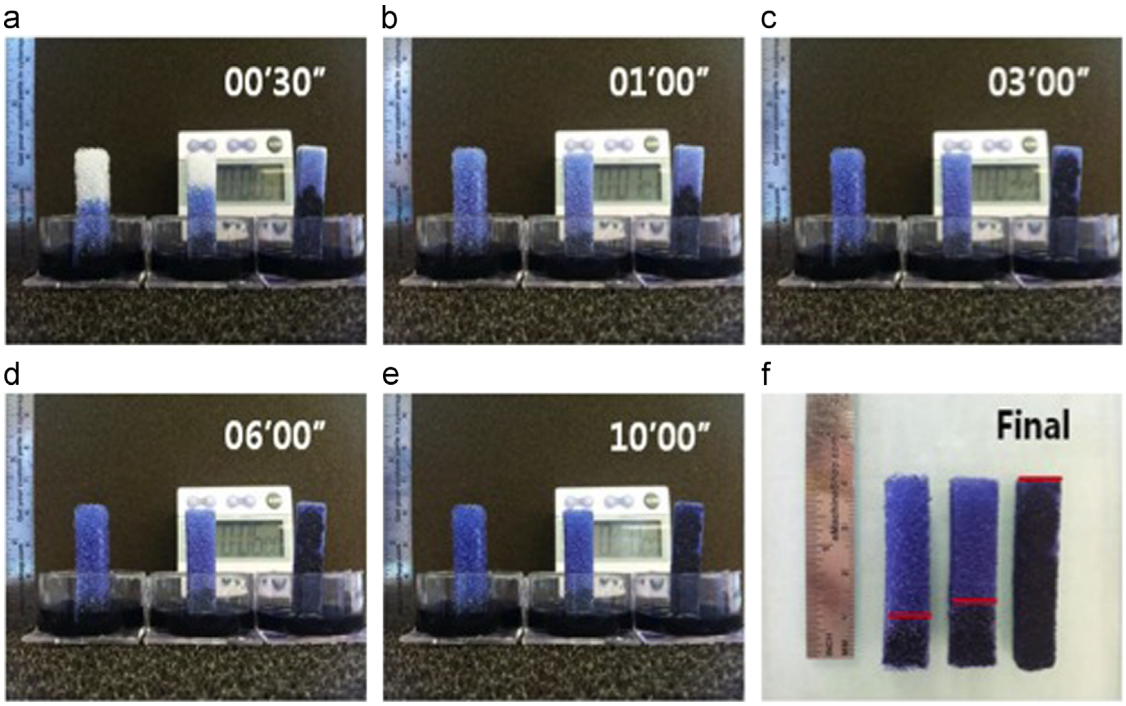

Fig. 5. Fluid heights for three different scaffold macro-pore sizes (a) at 30 s, (b) 1 min, (c) 3 min, (d) 6 min, and (e) 10 min. In (f) the final fluid height inside the three different sample scaffolds are shown. The left, the center, and the right specimens have 750 μm macro-pores with 50 μm micro-channels, 350 μm macro-pores with 50 μm micro-channels, and 150 μm macro-pores with 50 μm of micro-channels scaffold, respectively. Each picture shows different fluid heights in the macro-pores (dark stained region) and within the micro-channels (light stained region). (For interpretation of the references to color in this figure, the reader is referred to the web version of this article.)

compared to human allografts. However, to our knowledge, there is a lack of scientific explanation about the advantages of the micro-channeled scaffold in bone regeneration functions. In this study, we propose that capillary action, the anti-gravity physical phenomenon in nature, plays a major role in improving bone regeneration by enhancing the bone marrow absorption and retention. To elucidate our hypothesis, we created a mathematical model that predicted the height of fluid, absorption capability, in a scaffold tube after a certain amount of time based on a differential equation.

The mathematically estimated capillary heights for the four different scaffold tube diameters showed similar physical trends to the actual result heights, absorption capability, from the experiments: a scaffold with a smaller diameter tube outputs a greater capillary height that may imply strong absorption capability. Even though the mathematical formulation is based on an ideal situation, such as smooth surface roughness, and assumed various material properties and surface interface parameters, the numerically estimated values were very similar to those we obtained from the experimental

Table 2
Comparisons of the capillary height and time to maximum height between the mathematical prediction and scaffold experiment result.

Tube diameter (μm)	Maximum height		Time to maximum height	
	Mathematical prediction (mm)	Experimental data (mm)	Mathematical prediction (time to 90% of maximum height) (s)	Experimental data (s)
150/50	52	Over 40	30	~75
350/50	22	15	3	~2
750/50	10	10	0.3	~0.5

Note: Tube diameter represents the mean diameter of main pores in the scaffold structure. All these three different specimens are associated with 50 μm mean diameter of micro-channel of each trabecular.

data. The relationship between time and height in capillary action from the mathematical simulation was also consistent with the data we observed in the experiment. In other words, both the maximum height of the fluid and the rising rate of the fluid matched the mathematical predictions. These results support the interpretation of the physical role of the micro-channel inside the HA-scaffold by the capillary action. This study is truly a combination of physics and biology concerning the human body. Using a mathematical model to analyze a cellular response to a bone-like scaffold is a valid approach to tissue engineering and bone regeneration medicine. In order to obtain the optimal results in bone regeneration using the scaffold, we can mimic the capillary action, which can be learned from nature, to propel fluids against gravity.

From the experiments where we used three different macro-pore sized scaffolds, we also found that the smaller the pore size, the higher the fluid rose. However, the scaffold pore cannot be too small because it must provide enough space for cells to grow [14]. This is a trade-off situation when deciding the optimal pore size in the scaffold. By providing the micro-channels inside the scaffold struts, we could obtain both large enough macro-pore sizes as well as high capillary action.

Because multiple physical and material variables are involved in the equations that describe capillary action, these variables can be altered to produce the optimal conditions. If we can change the contact angle between the fluid and solid wall interface, the density of the fluid, and the pressure difference on the fluid interface, then we can control the optimized capillary height, thus improving the bone tissue regeneration function for large segmental defects. Change of the capillary speed and height can alternate the shear stress values on the tissue surfaces, which could enhance the cell in-growth rate.

There are several limitations in this study. First, the ideal capillary action was assumed and mathematically derived using a differential equation. Second, we did not consider any nano-pores inside the scaffold even though the real scaffold structure has countless nano-pores which will dramatically enhance the capillary action [14]. Third, the material and physical properties used in the numerical simulation did not perfectly match those used in the real micro-channeled HA-scaffold experiment. In the numerical simulation, we used the material properties of the blood, but media were used in the experiment. Fourth, we used a very simple straight scaffold tube in the mathematical simulation, but the real HA-scaffold is a complex three-dimensional structure. This means that our mathematical model is an ideal straight tube, but the real scaffold has large numbers of macro-pores and micro-channels in multiple directions. So, a direct comparison between the results from the mathematical model and experimental results is not possible. However, all of the above limitations do not violate the physical interpretations of our research results.

5. Conclusions

From this study, we confirmed our hypothesis, which states that capillary within the micro-channeled HA-scaffold not only increases fluid intake but also provides more space for cell habituation. The mathematically estimated fluid heights demonstrated a trend similar to that presented by the experiments. The capillary height could be increased with a smaller scaffold tube diameter. The experimental results confirmed the simulation results in the channels with micron-scale diameters in terms of not only the maximum fluid height but also the time for the fluid to reach the maximum height. We found that capillary action could be utilized to improve bone regeneration techniques through this micro-channeled HA-scaffold. As a further study, we would like to learn the manufacturing techniques of the scaffold specimen and perform experiments on cell proliferation. Our next research question is whether this innovative scaffold design can truly enhance bone regeneration capability inside a living body. However, to answer this question, in-vivo study is necessary. Finally, utilizing mathematical tools to study microscopic, physical phenomena and the following biological response can be revolutionary in tissue engineering.

References

[1] C. VanPutte, J. Regan, A. Russo, Seeley's Essentials of Anatomy and Physiology, 8th ed., McGraw-Hill, New York, 2012.
[2] J.S. Khurana, E.F. McCarthy, P.J. Zhang, Essentials in Bone and Soft-Tissue Pathology, Springer, New York, 2010.
[3] Arne Berner, Johannes C. Reichert, Michael B. Müller, Johannes Zellner, Christian Pfeifer, Thomas Dienstknecht, et al., Treatment of long bone defects and non-unions: from research to clinical practice, Cell Tissue Res. 347 (3) (2012) 501–519.

[4] M. Lappa, A Novel Approach for the Recognition, Definition and Characterization of the Critical Links between Fluid-dynamics and Soft Tissue Biomechanics, in: G.N. Greco (Ed.), Tissue Engineering Research Trends, Nova Science Publishers, New York, 2007, pp. 15–61.
[5] D.W. Hutmacher, Scaffolds in tissue engineering bone and cartilage, Biomaterials 21 (24) (2000) 2529–2543.
[6] K.F. Leong, C.K. Chua, N. Sudarmadji, W.Y. Yeong, Engineering functionally graded tissue engineering scaffolds, J. Mech. Behav. Biomed. Mater. 1 (2) (2008) 140–152.
[7] M.B. Fisher, R.L. Mauck, Tissue engineering and regenerative medicine: recent innovations and the transition to translation, Tissue Eng. Part B Rev. 19 (1) (2013) 1–13.
[8] J.R. Woodard, A.J. Hilldore, S.K. Lan, C.J. Park, A.W. Morgan, J. A. Eurell, et al., The mechanical properties and osteoconductivity of hydroxyapatite bone scaffolds with multi-scale porosity, Biomaterials 28 (1) (2007) 45–54.
[9] Juarez TM Goldstein AS1, C.D. Helmke, M.C. Gustin, A.G. Mikos, Effect of convection on osteoblastic cell growth and function in biodegradable polymer foam scaffolds, Biomaterials 22 (11) (2001) 1279–1288.
[10] R.E. Unger, A. Sartoris, K. Peters, A. Motta, C. Migliaresi, M. Kunkel, et al., Tissue-like self-assembly in cocultures of endothelial cells and osteoblasts and the formation of microcapillary like structures on three-dimensional porous biomaterials, Biomaterials 28 (27) (2007) 3965–3976.
[11] O. Gauthier, J.M. Bouler, E. Aguado, P. Pilet, G. Daculsi, Macroporous biphasic calcium phosphate ceramics: influence of macropore diameter and macroporosity percentage on bone ingrowth, Biomaterials 19 (1–3) (1998) 133–139.
[12] S.L. Ishaug-Riley, G.M. Crane, A. Gurlek, M.J. Miller, A.W. Yasko, M. J. Yaszemski, et al., Ectopic bone formation by marrow stromal osteoblast transplantation using poly (DL-lactic-co-glycolic acid) foams implanted into the rat mesentery, J. Biomed. Mater. Res. 36 (1) (1997) 1–8.
[13] G. Vunjak-Novakovic, L.E. Freed, Culture of organized cell communities, Adv. Drug Deliv. Rev. 33 (1–2) (1998) 15–30.
[14] D.S. Oh, Y.H. Kim, D. Ganbat, M.H. Han, P.H. Lim, J.H. Back, et al., Bone marrow absorption and retention properties of engineered scaffolds with micro-channels and nano-pores for tissue engineering: a proof of concept, Ceram. Int. 39 (2013) 8401–8410.
[15] P.K. Kundu, I.M. Cohen, D.R. Dowling, Fluid Mechanics, Academic Press, 5th ed., Waltham, 2011, pp. 8-12.
[16] Science Encyclopedia, Capillary action. ⟨http://science.jrank.org/pages/1182/Capillary-Action.html/⟩. Accessed 20 Sep 2013.
[17] Quora, Water: what makes water unique. ⟨http://www.quora.com/Water/What-makes-water-unique/⟩. Accessed 20 Sep 2013.
[18] J. Siggers, Physiological Fluid Mechanics Lecture note. ⟨http://www.bg.ic.ac.uk/research/j.siggers/physiologicalfluids_shortcourse.pdf/⟩. Accessed 20 Sep 2013.
[19] Y.A. Cengel, J.M. Cimbala, in: Fluid Mechanics: Fundamentals and Applications, McGraw-Hill, New York, 2006, p. 51–56.
[20] H. Bruus, Theoretical Microfluidics, Oxford University Press, Oxford, 2006, p. 91–100 (Lecture note).